International Journal of Biochemistry and Cell Biology 103 (2018) 81–88

Contents lists available at ScienceDirect

International Journal of Biochemistry and Cell Biology

journal homepage: www.elsevier.com/locate/biocel

Blue light emitting diodes irradiation causes cell death in colorectal cancer by inducing ROS production and DNA damage

Gege Yan[a,c,1], Lai Zhang[a,c,1], Chao Feng[a,c,1], Rui Gong[a,c], Elina Idiiatullina[f], Qihe Huang[a,c], Mingyu He[a,c], Shuyuan Guo[d], Fan Yang[a,c], Yuan Li[a,c], Fengzhi Ding[a,c], Wenya Ma[a,c], Valentin Pavlov[e], Zhenbo Han[a,c], Zhiguo Wang[a,c], Chaoqian Xu[e], Benzhi Cai[b,c], Ye Yuan[a,c,*], Lei Yang[b,**]

[a] Department of Clinical Pharmacy, The Second Affiliated Hospital of Harbin Medical University, Harbin, 150086, China
[b] Department of Orthopedics, The First Affiliated Hospital of Harbin Medical University, Harbin, 150001, China
[c] Department of Pharmacology, College of Pharmacy, Harbin Medical University, Harbin, 150081, China
[d] Department of Cardiology, The First Affiliated Hospital, Cardiovascular Institute, Harbin Medical University, Harbin, 150001, China
[e] Department of Pharmacology, College of Pharmacy, Mudanjiang Medical University, Mudanjiang, 157011, China
[f] Central Laboratory of Scientific Research, Bashkir State Medical University, Ufa, 450008, Russia

ARTICLE INFO

Keywords:
Blue LED light
Colorectal cancer (CRC)
Reactive oxygen species (ROS)
Apoptosis
DNA damage
Epithelial-mesenchymal transition (EMT)

ABSTRACT

The light emitting diodes (LEDs) irradiation has been demonstrated to be potential therapeutic strategies for several diseases. However, the blue LED effects remain largely unknown in colorectal cancer (CRC), which is a major cause of morbidity and mortality throughout the world. In this study, we determined the effects of blue LED irradiation, the maximal light emission at 470 nm in wavelength, in human CRC cell lines SW620 and HT29. The cells were irradiated with blue LED light for 0 J/cm^2, 72 J/cm^2, 144 J/cm^2, 216 J/cm^2 and 288 J/cm^2 respectively. We found that irradiation with blue LED light induced a marked decrease of live cells and an increase of dead cells. Additionally, lower cell proliferation and a remarkably increase of cell apoptosis were observed in blue LED-irradiated cells as compared with non-irradiated control group. The cell migration was significantly inhibited by blue LED irradiation 24, 48 and 72 h later compared with non-treated group. Blue LED-treated CRC cells further displayed a remarkably inhibition of EMT process in CRC cells. Finally, we found the accumulation of ROS production and DNA damage were induced by blue LED irradiation. These results indicated that blue LED irradiation inhibits CRC cell proliferation, migration and EMT process as well as induces cell apoptosis, which may result from increased ROS accumulation and induction of DNA damage.

1. Introduction

Colorectal cancer (CRC) is one of the most commonly cancers worldwide, which occurs in the colon or rectum. An estimated 1,361,000 people are diagnosed with CRC annually (Rabeneck et al., 2015). It is causally associated with a combination of genetic and environmental factors (Wei et al., 2004). General treatments used for CRC patients include some combination of surgery, radiation therapy, chemotherapy and targeted therapy (Hollande et al., 2010). Despite substantial progress in the treatment of CRC, the prognosis for patients of the disease remains poor (Markowitz and Bertagnolli, 2009).

Light emitting diode (LED)-based light therapy has grown in popularity in the past few years, which is a painless, relaxing, non-invasive biophysical and highly effective treatment for several diseases (Barolet et al., 2009; Neupane et al., 2010; Oshima et al., 2011; Stelian et al., 1992; Teuschl et al., 2015). However, the LED light has been widely and successfully used in the red and near infrared ranges (Fonseca et al., 2013; Giacci et al., 2015; Karu, 2008; Li et al., 2014; Takhtfooladi et al., 2015). To date, studies showed that these lights have positive effects on injured cells triggering an instant response to create adenosine triphosphate (ATP), which is cellular energy (Benedicenti et al., 2008; Wang et al., 2015). It also has shown to increase both DNA and RNA functions (Gao and Xing, 2009). More recently, at wavelengths ranging from 400 to 500 nm, blue LED light has

* Corresponding author at: Department of Clinical Pharmacy, The Second Affiliated Hospital of Harbin Medical University, Harbin, 150086, China.
** Corresponding author at: Department of Orthopedics, The First Affiliated Hospital of Harbin Medical University, Harbin, 150001, China.
E-mail addresses: yuanye_hmu@126.com (Y. Yuan), yangray83@vip.qq.com (L. Yang).
[1] Equal contributors to this work.

https://doi.org/10.1016/j.biocel.2018.08.006
Received 30 March 2018; Received in revised form 23 July 2018; Accepted 15 August 2018
Available online 17 August 2018
1357-2725/

been shown to regulate cell growth, proliferation and apoptosis in some cancer cells and non-cancer cells, such as B-cell lymphoma (Oh et al., 2016), melanoma (Oh et al., 2015), skin tumors (Ohara et al., 2003) retinal neuronal cells (Knels et al., 2011) and skin dermal fibroblasts (Mamalis et al., 2015) by regulating autophagy, reactive oxygen species (ROS) production and mitochondrial mediated signaling pathways. Despite its functional importance in various fundamental bioprocesses, the studies of blue LED irradiation on CRC cells have been still limited. Accordingly, our study demonstrated that the functional importance of blue LED irradiation on CRC cell growth, apoptosis and migration, which provided profound insights into CRC therapy in the future.

2. Materials and methods

2.1. Culturing of colon adenocarcinoma cell lines

Human colon adenocarcinoma cell lines SW620 and HT29 were obtained from ATCC (Manassas, Virginia, USA). These cells were cultured in RPMI-1640 medium supplemented with 10% fetal bovine serum (FBS) (Embriolife®, Vitrocell, Brazil) and antibiotics (penicillin 100 U/mL and streptomycin 100 mg/mL). Cells were maintained at 37°C in a water-saturated atmosphere with 5% CO_2.

2.2. Blue LED irradiation, Irinotecan treatment and cell counting assay

Cells were irradiated one day after plating by using a blue LED light (470 nm) at a power density of 20 mW/cm^2 for 72 J/cm^2, 144 J/cm^2, 216 J/cm^2 and 288 J/cm^2 respectively at room temperature. The cells were vertical under the blue light source with the distance of 31.5 cm. Besides, cells were subjected to Irinotecan (IT) (MOLBASE, Shanghai, China, 97682-44-5) at the concentration of 25 μM for 24 h when the degree of cell confluence reaches 70%. After that, the cells were stained with Trypan Blue and counted using count star easy cell analysis (Count star, Shang Hai, China) to detect the number of live cells and the rate of dead cells.

2.3. Ethynyl-2-deoxyuridine (EdU) cell proliferation assay

The EdU cell proliferation assay was described previously (Cai et al., 2016) using an EdU Apollo DNA in vitro kit (Ribobio, Guang Zhou, China) according to the manufacturer's protocol. Briefly, cells were fixed with 4% paraformaldehyde (m/v) for 30 min and then incubated with 50 μM EdU at 37°C for 2 h. After the cells were permeabilized in 0.5% Triton X-100, they were added to Apollo staining solution and incubated in a shaker for 30 min in the dark. Finally, the cells were incubated with 20 μg/mL 4',6-diamidino-2-phenylindole (DAPI) for 10 min. The EdU index (%) was the average ratio of the number of EdU-positive cells to total cells in randomly selected areas under a fluorescence microscope (IX73P1F, Olympus Optical, Tokyo, Japan). Cores ≥10 cells were included in the analysis.

2.4. Apoptosis assay

Cells were cultured for 24 h after irradiation with blue LED light for 144 J/cm^2 or no irradiation. The percentages of apoptotic cells were measured using Annexin V-FITC staining (Beyotime Biotechnology, Shang Hai, China) by flow cytometry (Guava PCA, Merck Millipore, Billerica, Massachusetts, USA). Briefly, cells were washed twice with cold PBS and re-suspended at a concentration of 1×10^6 cells/mL in 100 μL binding buffer. After staining with Annexin V-FITC, cells were analyzed by flow cytometry (Guava PCA, Millipore). Ten thousand cells were acquired and data were processed by the software FCS Express V3 (De Novo Software, Los Angeles, CA, USA).

2.5. Antigen Ki67 and γ-H2 A.X immunostaining

γ-H2 A.X immunostaining was used to detect DNA double-strand breaks (DSBs). Ki67 immunostaining was applied to test cell proliferation. Cells were fixed using 4% paraformaldehyde (m/v) and permeabilized using a 0.3% Triton X100 solution. The cells were then incubated in PBS supplemented with 0.1% Tween and 2% fetal bovine serum (FBS) (Embriolife®, Vitrocell, Brazil) for 1 h. Cells positive for γ-H2 A.X were detected using mouse anti γ-H2 A.X phospho S139 (200× diluted, ab26350, Abcam, Cambridge, UK). Cells positive for Ki67 were determined by a rabbit anti Ki67 (200× diluted, 9129, Cell Signaling Technology, USA). A secondary incubation step was performed using Alexa Fluor® 594 goat anti-mouse (200× diluted, ab150116, Abcam) and Alexa Flour® 488 Conjugate anti-rabbit (200× diluted, 5429, Cell Signaling Technology). After a PBS wash, the cells were progressively dehydrated with alcohol, and then, nuclear staining was performed with DAPI (2.5 μg/mL). Fluorescence signals were visualized under a confocal laser scanning microscope (FV10i, Olympus Optical).

2.6. Western blot

This assay was described previously (Ma et al., 2018). Cells were lysed in cell lysis buffer (P0013B, Beyotime Biotechnology) supplemented with PMSF protease inhibitor. Protein concentration was measured using the BCA Protein Assay Kit (P0010S, Beyotime Biotechnology). 70 μg protein was separated on a polyacrylamide gel and transferred to a nitrocellulose membrane. The membrane was incubated overnight at 4°C with primary antibodies diluted in PBS with rabbit monoclonal antibodies of anti-TWIST1 (1,000× dilution, 18125-1-AP, Proteintech, Chicago, USA); anti-N-Cadherin (1,000× dilution, 13116); anti-E-Cadherin (1,000× dilution, 3195); anti-Vimentin (1,000× dilution, 5741); and mouse monoclonal antibody of anti-GAPDH (1,000× dilution, OTI2D9, ZSGB-BIO, Beijing, China). A secondary incubation step was carried out with anti-rabbit IgG (5,000× dilution, 14708, rabbit monoclonal antibody) or anti-mouse IgG (5,000× dilution, 3420, mouse monoclonal antibody). The rest antibodies without mention of companies were purchased from Cell Signaling Technology. The western blot bands were collected by odyssey CLx and quantified with LI-COR Image Studio Software (LI-COR Biosciences, Lincoln, NE). The results were expressed as fold changes by normalizing the data to the control GAPDH values.

2.7. Quantitative reverse transcription polymerase chain reaction (qRT-PCR)

Total RNA was extracted using TRIzol reagent (Life technologies, CA, USA) according to the manufacturer's instructions. Briefly, 500 ng total RNA was reverse transcribed to cDNA in a total reaction volume of 10 μL with High Capacity cDNA Reverse Transcription Kit (Thermo Fisher Scientific, USA). Further analysis was performed with 1 μL cDNA using SYBR Green PCR Master (Rox) (Roche, Basel, Switzerland) in a 7500 Fast Real-Time instrument (Applied Biosystems, Foster City, CA, USA). Relative expression was evaluated using the comparative CT method and normalized to endogenous GAPDH mRNA. E-cadherin Forward primer: GATAATCCTCCGATCTTCAATCCC; E-cadherin Reverse primer: CAATATGGTGTATACAGCCTCCC. Vimentin Forward primer: TTTGAAGAAACTCCACGAAGAGGA; Vimentin Reverse primer: CCACATCGATTTGGACATGCT.

2.8. Measurement of reactive oxygen species (ROS) production

Intracellular levels of ROS production were measured using a Reactive Oxygen Species Assay Kit (S0033, Beyotime Biotechnology) according to the manufacturer's instructions. After washing three times with PBS, cells were incubated with 10 μM DCFH-DA probes for 30 min at 37°C. Following the removal of the superfluous DCFH-DA probes that

did not penetrate into CRCs, the cells were fixed in 4% paraformaldehyde (m/v) for 30 min and stained with DAPI (20 μg/mL) for 10 min. The cells were imaged with a fluorescence microscope (Olympus Optical). Cores ≥10 cells were included in the analysis.

2.9. Cell migration assay

A scratch assay was done to assess cell migration. An artificial wound was created before irradiation by blue LED light using a sterile 200 μL pipette tip on the confluent cell monolayer in 6-well plate. To visualize migrated cells, images were taken at 0, 24, 48 and 72 h after treatment. The rate of wound closure was performed with Image J software (NIH, USA).

2.10. Statistical analysis

All assays were repeated at least three times, and values were given as the mean ± SEM. Statistical analysis was performed by one-way analysis of variance (ANOVA) followed by Dunnett's Multiple Comparison test (GraphPad Software Inc., San Diego, CA) for cell counting assays. For two-group comparisons, the Shapiro-Wilk test was used for normality test (22.0.0.0 version, IBM, Armonk, New York, USA). Student's unpaired *t*-test was used for normal distributed data and Mann-Whitney *U* test was performed for non-normally distributed data. P values < 0.05 were considered statistically significant.

3. Results

3.1. Inhibition of CRC cells growth upon blue LED irradiation

The maximal light emission of the blue LED light is at a 470 nm wavelength shown previously (Yuan et al., 2017). We examined the effect of blue (peaked at 470 nm) and red (peaked at 630 nm) LED irradiation on CRC cell growth. SW620 and HT29 cells were exposed to LED light for 0 J/cm^2, 72 J/cm^2, 144 J/cm^2, 216 J/cm^2 and 288 J/cm^2 respectively, and subsequently cell growth was evaluated by Trypan Blue staining and then analyzed by cell counting assays. The obvious shrinkage and rounding of the cells were observed upon treatment with blue LED irradiation for more than 144 J/cm^2 in both cell lines compared with non-irradiated control group (Fig. 1A). However, no significant differences were seen between irradiation for 72 J/cm^2 and non-irradiated control group. Moreover, significant changes of live and dead cell numbers were upon treatment with blue LED irradiation for at least 144 J/cm^2 or 216 J/cm^2 in both cell lines (Fig. 1B and C). With blue LED irradiation for 288 J/cm^2, the average percentages of dead cells were increased maximally to 45% and 61% in SW620 and HT29 cell lines respectively. However, as the results shown in Fig. 1D–F, it shows no effect of red LED irradiation on colorectal cell growth, indicating this effect was specific upon irradiation with blue LED lights in CRC cells.

To further compare the effects of treatments between blue LED and irinotecan (IT), a DNA topoisomerase poison. Both treatments cause cell death in SW620 and HT29 CRC cell lines. Besides that, blue LED irradiation with 144 J/cm^2 induced a more cell death effects than IT treatments in both cell lines (Fig. 1H and I).

3.2. Inhibition of proliferation and induction of apoptosis in blue LED irradiated CRCs

To further investigate the effects of blue LED irradiation on CRC cell proliferation, the EdU staining and Ki67 staining were employed to determine the percentages of EdU-positive and Ki67-positive cells after blue LED irradiation for 0 J/cm^2 or 144 J/cm^2. A decrease of percentages of proliferative cells was observed after irradiation with blue LED lights compared with non-irradiation control groups. The percentages of EdU-positive cells have reduced from around 27% to 1% in SW620 and from 10% to 5% in HT29 (Fig. 2A and B). Similar results were observed in Ki67 staining assay (Fig. 2C and D). Blue LED irradiation also reduced the percentages of ki67 positive cells in both SW620 and HT29 CRC cell lines. These results indicated that blue LED irradiation significantly inhibits CRC cell proliferation.

Based on Annexin V-FITC staining, the percentages of apoptotic cells were significantly increased in both SW620 and HT29 cell lines upon 144 J/cm^2 of irradiation of blue LEDs compared with non-irradiated control group (Fig. 3A and B). We also explored the expression levels of apoptosis-related proteins Bax and Bcl-2 by Western blot. As shown in Fig. 3C, the results indicated that blue LED irradiation resulted in an increase of apoptotic Bax, whereas a decrease of anti-apoptotic Bcl-2. Thus, blue LED irradiation leads to a decrease of proliferative CRC cells and an increase of apoptotic cells.

3.3. Inhibition of migration and epithelial–mesenchymal transition (EMT) of CRC cells with blue LED irradiation

Cell migration and invasion are implicated in the pathophysiology of many diseases, especially cancers (Bozzuto et al., 2010). We performed a scratch assay in monolayer cells to identify the effects of blue LED irradiation on CRC cell migration. As shown in Fig. 4, blue LED irradiation resulted in a significant reduction of cell migration in both SW620 and HT29 cell lines. Cell migration began to reduce starting at 24 h and 48 h after treatments for SW620 and HT29 respectively, which revealed that blue LED irradiation significantly inhibits CRC cell migration.

An epithelial-mesenchymal transition (EMT) is a biologic process leading eventually invasion and metastasis in cancers (Kalluri and Weinberg, 2009). To further determine the effects of blue LED irradiation on EMT process, we analyzed the expression levels of markers associated with EMT upon blue LED irradiation in SW620 and HT29 cell lines. Western blot analysis showed that blue LED irradiation led to a remarkable increase in expression of epithelial marker E-cadherin as well as decreases of mesenchymal markers expression of N-cadherin, Vimentin and TWIST1 in SW620. However, the effects were a litter bit weaker in HT29. E-cadherin and TWIST1 have relative slight changes after treatment with blue LEDs in HT29 (Fig. 5A). In addition, qRT-PCR analysis also revealed a significant increase in gene expression of E-cadherin, whereas decrease in Vimentin (Fig. 5B). Taken together, these findings demonstrated a significant inhibition of migration and EMT process of CRC cells by blue LED irradiation.

3.4. Increase of intracellular reactive oxygen species (ROS) levels in CRCs upon blue LED irradiation

Reactive oxygen species (ROS) can influence many central cellular processes such as proliferation, apoptosis and senescence which are implicated in the development of cancer (Waris and Ahsan, 2006). We performed DCF-DA staining to further evaluate effects of blue LED irradiation on ROS production in comparison to non-treated CRC cell group. Blue LED irradiation significantly induced elevation of ROS production in both the nucleus and the cytoplasm, (Fig. 6A) which led to a significant increase of ROS-positive cells percentages by 95.9% and 48.2% in SW620 and HT29 cell lines respectively (Fig. 6B). These findings indicated that blue LED irradiation is able to induce intracellular ROS generation in CRCs.

3.5. Blue LED irradiation leads to DNA damage in CRC

Phosphorylation of the Ser-139 residue of the histone variant H2 A.X, forming γ-H2 A.X, is an early cellular response to the induction of DNA double-strand breaks (Mah et al., 2010). We therefore investigated if blue LED irradiation caused DNA damage in CRC cells using γ-H2 A.X immunostaining. As compared with those in non-irradiated control groups, the percentages of γ-H2 A.X positive cells were

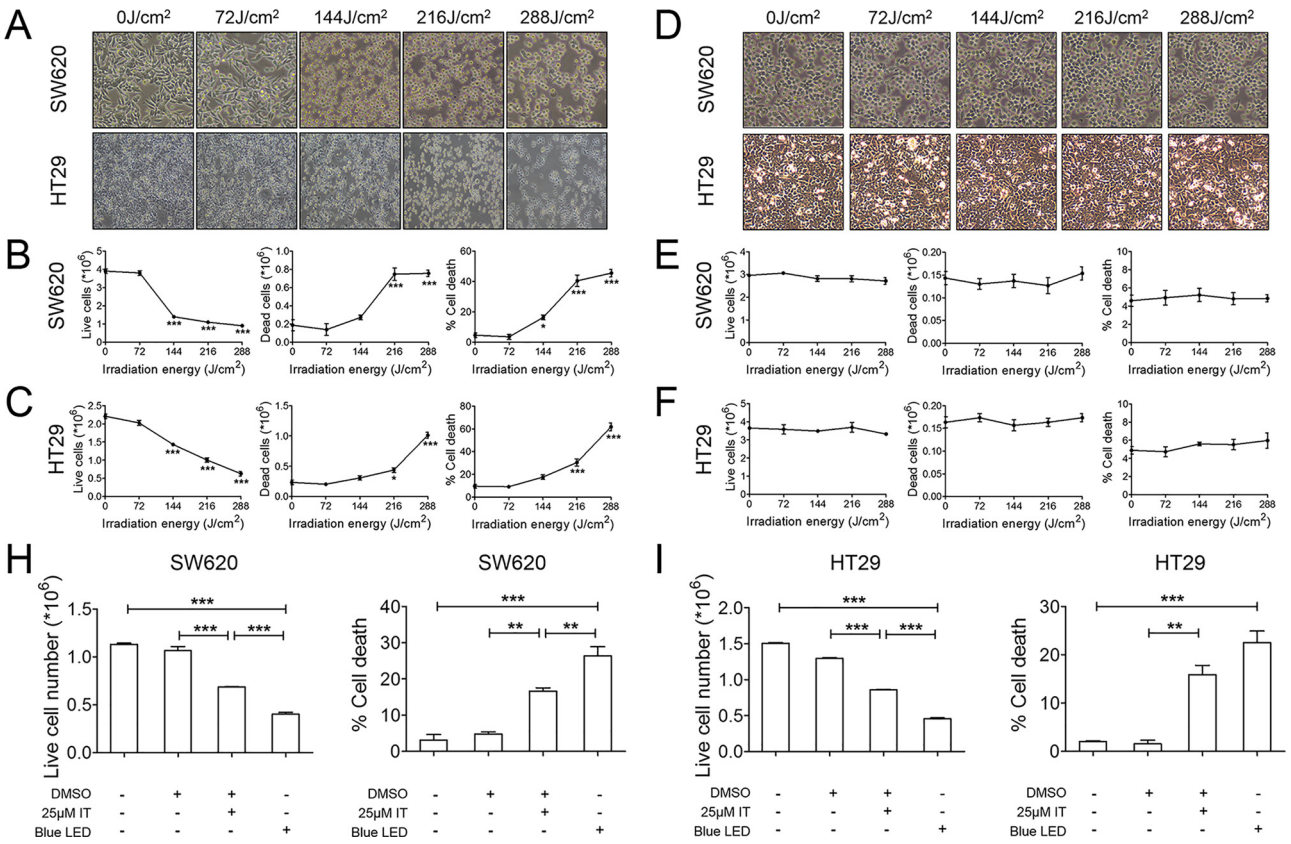

Fig. 1. The effects of blue LED irradiation on CRC cell growth. Following (A, B) blue LED and (C, D) red LED irradiation, CRC cells were stained with Trypan Blue and determined by cell counting assay. (A, E) Representative images taken under a microscope (magnification × 40). The panels show the number of live cells and dead cells as well as the percentages of dead cells in (B, E) SW620 and (C, F) HT29 cell lines. (H, I) Comparison effects between blue LED and Irinotecan (IT) treatments on cell growth of SW620 and HT29 cell lines. N = 3; $*P < 0.05$; $***P < 0.001$.

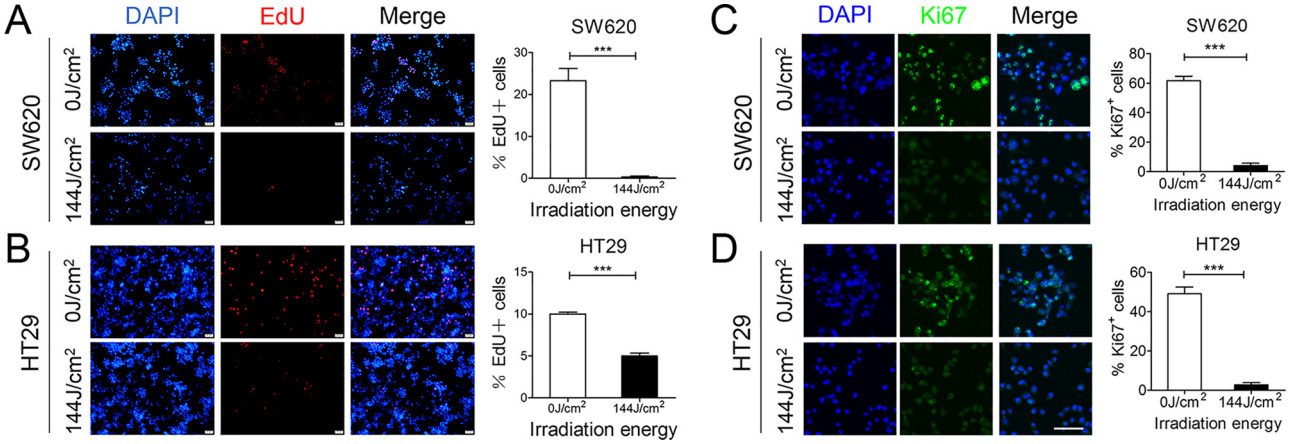

Fig. 2. Anti-proliferative effects of blue LED light exposure on CRC cells. CRC cells were treated with blue LED irradiation for 0 J/cm^2 and 144 J/cm^2. (A, B) An ethynyl-2-deoxyuridine (EdU) staining assay was performed to assess CRC cell proliferation. Representative immunofluorescence staining of (A) SW620 and (B) HT29. Shown are DAPI (blue), EdU (red) and merged images. Photos of the selected areas were taken randomly under fluorescence microscopy. The panels show percentages of the EdU-positive cells in (A) SW620 and (B) HT29. (C, D) Representative epifluorescence images of (C) SW620 and (D) HT29 with Ki67 (green) and DAPI (blue), and the panels show the percentage of Ki67 positive cells. N = 5; $***P < 0.001$. Bar: 100 μm.

significantly increased in the groups of blue LED irradiation (Fig. 6C). After irradiation for 144 J/cm^2, we observed a marked increase in DNA damaged cells of 25.3% SW620 cells and 27.3% HT29 cells respectively (Fig. 6D). Together, these results indicate that blue LED irradiation resulted in an increased DNA damage in CRC cells.

4. Discussion

In this study, we investigated the effects of blue LED irradiation with maximal light emission at 470 nm in wavelength on CRC cells. The results demonstrated blue LED irradiation inhibited CRC cell proliferation, migration and EMT process as well as induced apoptosis. Their underlying mechanisms are associated with the increased ROS production and DNA damage.

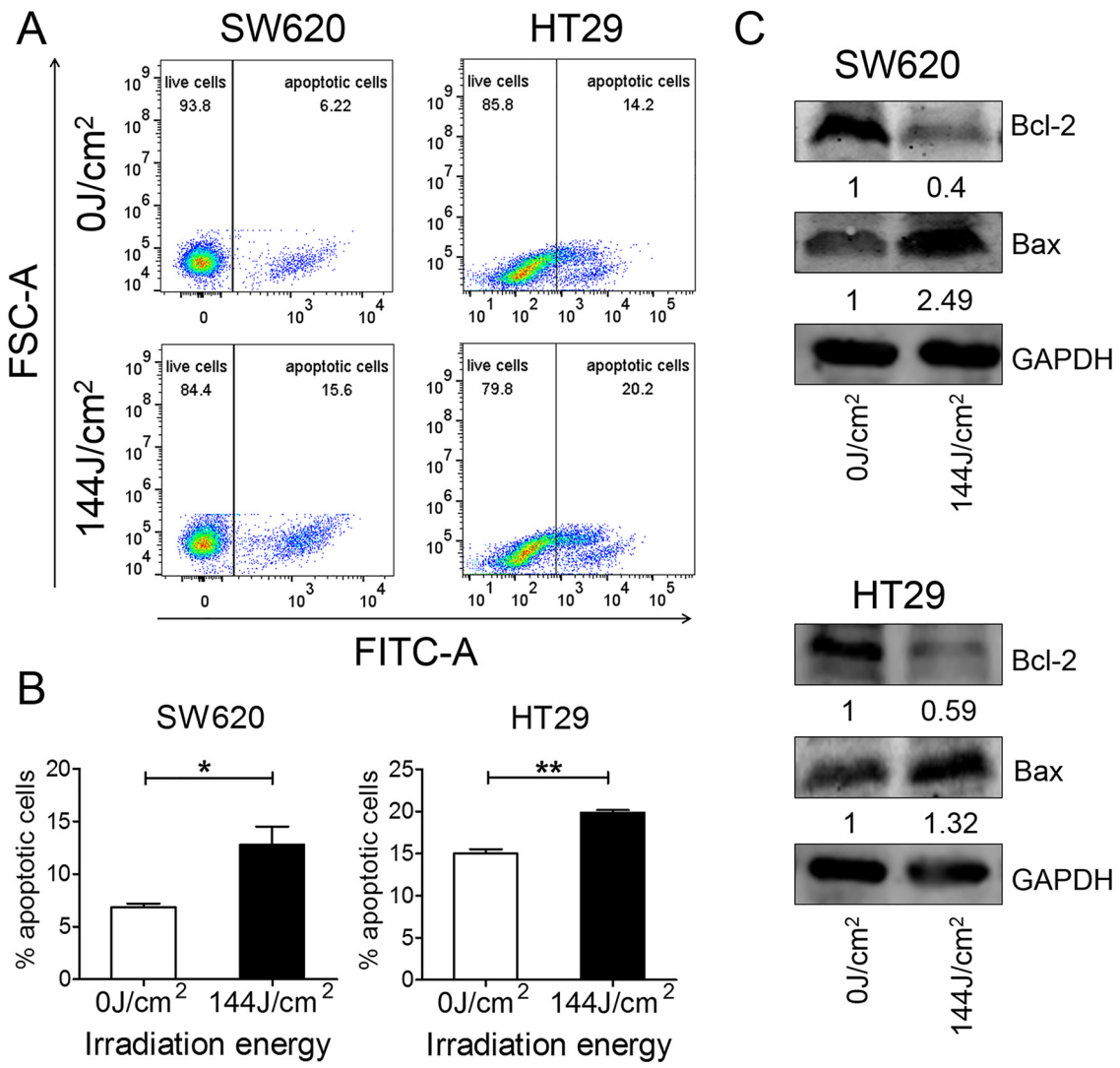

Fig. 3. Pro-apoptotic effects of blue LED irradiation on CRC cells. The percentages of apoptotic CRC cells were stained by Annexin V-FITC and determined by flow cytometry upon irradiation with blue LED. (A) Representative images of analyzed results of flow cytometry after Annexin V-FITC staining in both SW620 and HT29 cell lines. (B) The panels show percentages of apoptotic cells in SW620 and HT29. (C) Western blot was performed to detect the protein levels of Bcl-2 and Bax in SW620 and HT29 after exposed to blue LED irradiations for 0 J/cm^2 and 144 J/cm^2. They were normalized to GAPDH. N = 3; *$P < 0.05$; **$P < 0.01$.

Previous reports demonstrated mitochondrial membrane potential in blue LED-irradiated cells. They showed a loss of mitochondrial membrane potential the presence of damaged mitochondrial membrane after irradiation with blue LED (Oh et al., 2016). In addition, Argun et al. observed that blue light induced a significant increase in intracellular Ca^{2+} levels in ARPE-19 cells (Argun et al., 2014). Here, we showed that an increase of ROS production and DNA damage was associated with negative effects of blue LED irradiation on CRC cells. Interestingly, they also found blue light induced ROS accumulation and cell apoptosis in their studies, which were similar with the results in our study. Whilst blue light has been proven to delay cell division and DNA synthesis of cells (Oldenhof et al., 2004). And in another study, Chui et al. have determined that the blue LED irradiation did lead to a remarkably decreased expression of genes associated with chromosomal DNA replication and cell division (Chui et al., 2012). Therefore, we assumed that the effects of blue LED light on CRCs might be caused by an increase of mitochondrial membrane potential and intracellular Ca^{2+} levels as well as a decrease of cell division.

As we know, many oncogenes and tumor suppressor genes have been reported to casually link to the development of CRC. For example, TGF-β mediated activation of MEK-Erk and p38-MAPK pathways combined with SMAD4 loss have been directly correlated with CRC metastasis (Papageorgis et al., 2011). Damage Specific DNA Binding Protein 2 (DDB2) suppresses EMT process in CRC cells (Roy et al., 2013). The novel long noncoding RNA TUSC7 inhibits proliferation by sponging miR-211 in CRCs (Xu et al., 2017). These findings generally suggested a complicated multifactorial process involved in the regulation of the CRC development. While in our study, we found increased ROS accumulation and induction of DNA damage after blue LED irradiation. In theory, ROS can be produced in the mitochondria via the electron transport chain. Additionally, ROS levels can be increased dramatically by exogenous sources, such as ultra violet (UV). In a study, they determined UV exposure induces DNA breakdown and causes cellular damage through the production of ROS leading to programmed cell death in retinal pigment epithelium ARPE19 cells (Roduit and Schorderet, 2008). More importantly, several studies showed the ROS accumulation are able to promote tumor progression via regulating some oncogenes or tumor suppressor genes expression. Ju et al., found the accumulation of ROS induced by luteolin resulted in suppression of NF-κB and potentiation of JNK to sensitize lung cancer cells to undergo TNF-induced apoptosis (Ju et al., 2007). Levistolide A has been demonstrated to induced CRC apoptosis via ROS mediated endoplasmic reticulum (ER) stress pathway (Yang et al., 2017). Therefore, we assumed the effects of blue LED irradiation on CRC cells might be

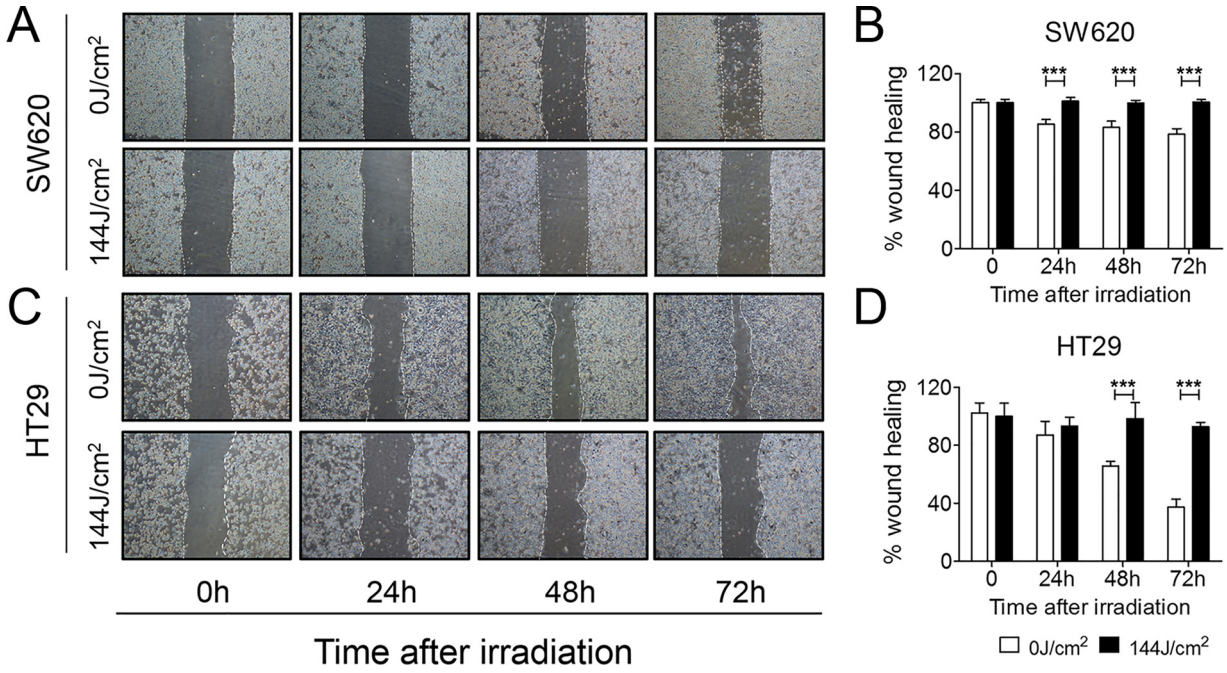

Fig. 4. Inhibition effects of blue LED irradiation on CRC migration. Scratch assay was performed on confluent SW620 and HT29 cells and migration into the wound was monitored for 24, 48 and 72 h under microscopy. (A, B) Representative images of scratch assays at the initial time of scratch (0 h) and after 24, 48 and 72 h in SW620 and HT29 cell lines. Bar graphs show the relative cell migration efficiency after blue irradiation over time in (C) SW620 and (D) HT29 cell lines. N = 5; $*P < 0.05$; $**P < 0.01$.

associated with regulation of some oncogenes/tumor suppressor genes.

Our previous study has demonstrated the toxic effects of blue LED irradiation on bone marrow-derived mesenchymal stem cells (BMSCs) (Yuan et al., 2017). Blue LED irradiation also induced increases of ROS production and DNA damage in BMSCs. Thus, we assume the toxic effects of blue LED irradiation were actually non-specific for cancer cells. However, the sensitivity to the effects was much different for various types of cells. Niu et al. showed combination of curcumin with blue LED light united red light irradiation can attain a higher efficiency of regulating cell proliferation and apoptosis in skin keratinocytes (Niu et al., 2015). Thus, it is necessary to investigate whether irradiation with a combination of different LED colors will have synergistic effects with medical treatments or drugs on CRC cells. Further studies are needed to elucidate the effects of LEDs with different wavelengths, which may produce different effects and to determine the molecular mechanisms of these effects.

In summary, our study provided a direct evidence that blue LED irradiation has inhibited effects on CRC cells, which characterized by inhibition of CRC cell growth, proliferation, migration and EMT process as well as induction of cell apoptosis. It might be caused by induced ROS production and DNA damage. Collectively, these findings provided a novel potential therapeutic strategy for CRC in the future.

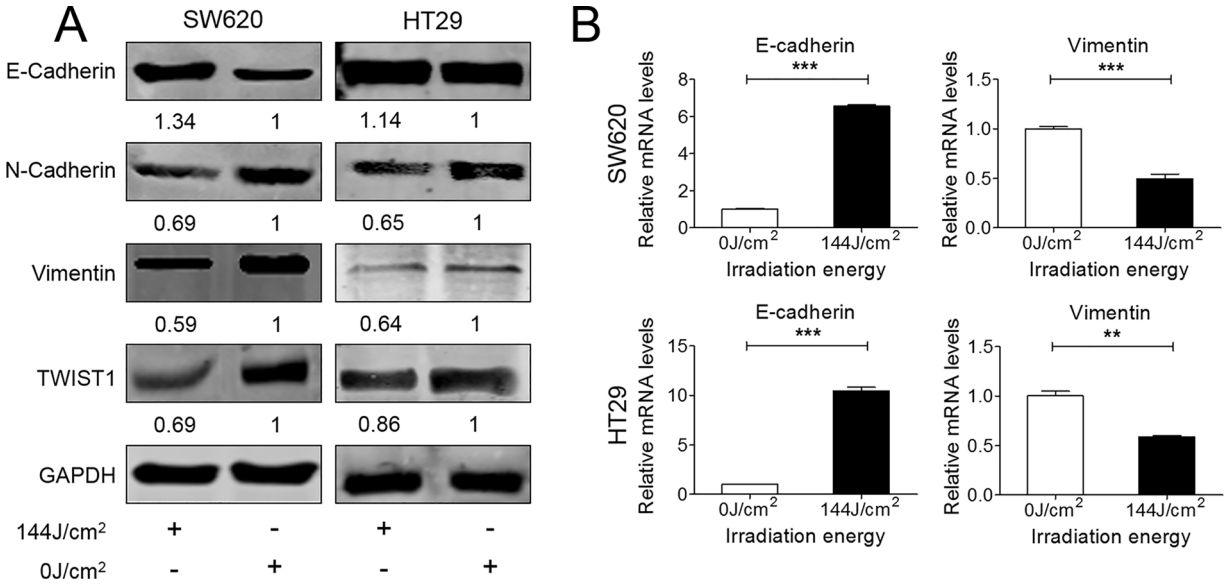

Fig. 5. Inhibition of EMT in CRC cells with blue LED irradiation. (A) Western blot analysis of EMT markers E-cadherin, N-cadherin, Vimentin and TWIST1 were shown in (left) SW620 and (right) HT29 CRC cell lines respectively. (B) E-cadherin and Vimentin mRNA expression in (above) SW620 and (below) HT29 following the irradiations of blue LED for 0 J/cm^2 and 144 J/cm^2. Data are expressed as the mean ± SEM. *P < 0.05; **P < 0.01; ***P < 0.001.

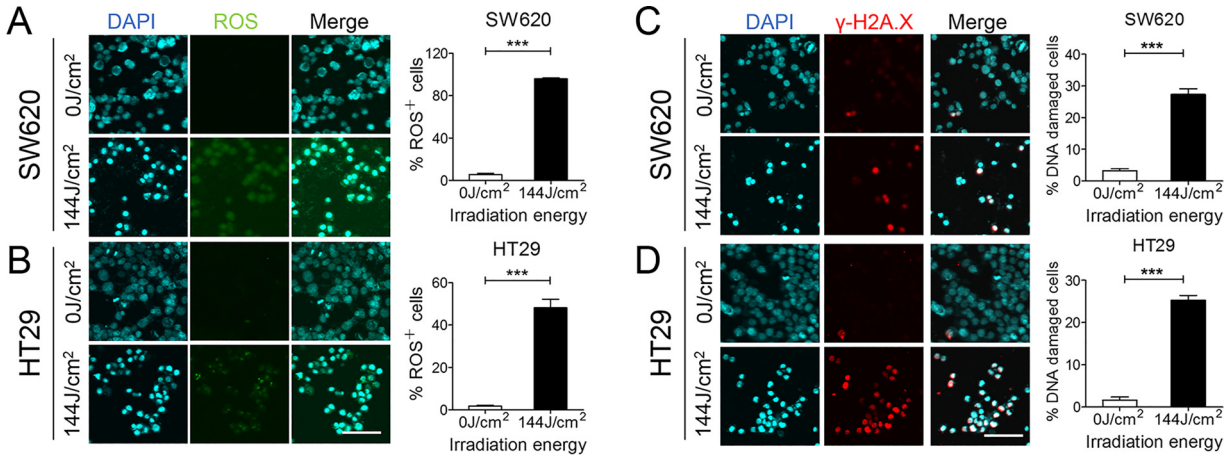

Fig. 6. Effects of blue LED light on generation of ROS and DNA damage in CRC cells. Peroxide-sensitive fluorescent probe, DCFH-DA staining was used to measure intracellular levels of ROS production in CRCs under blue LED irradiation. (A, B) Representative immunofluorescence staining of CRC cells. Shown are DAPI (blue), ROS (green) and merged images in (A) SW620 and (B) HT29 cell lines. Photos were taken randomly. The panels show the percentages of ROS-positive cells in (A) SW620 and (B) HT29. N = 6; ***P < 0.001. (C, D) γ-H2A.X immunostaining followed by confocal microscopy was used to determine the status of DNA damage in CRCs irradiated by blue LED. Representative immunofluorescence staining of CRC cells. Shown are DAPI (blue), γ-H2A.X (red) and merged images in (C) SW620 and (D)HT29 cell lines. Photos were taken randomly. The panels show the percentages of γ-H2A.X positive cells in (C) SW620 and (D) HT29. N = 6; ***P < 0.001. Bar: 100 μm.

Disclosure of potential conflicts of interest

The authors indicate no potential conflicts of interest.

Acknowledgments

This work was supported by grants from The National Key Research and Development Program of China (2017YFB0403802), the National Natural Science Fund of China (81603146), China Postdoctoral Science Foundation (2018M630365).

References

Argun, M., Tok, L., Uguz, A.C., Celik, O., Tok, O.Y., Naziroglu, M., 2014. Melatonin and amfenac modulate calcium entry, apoptosis, and oxidative stress in ARPE-19 cell culture exposed to blue light irradiation (405 nm). Eye (Lond.) 28 (6), 752–760.
Barolet, D., Roberge, C.J., Auger, F.A., Boucher, A., Germain, L., 2009. Regulation of skin collagen metabolism in vitro using a pulsed 660 nm LED light source: clinical correlation with a single-blinded study. J. Invest. Dermatol. 129 (12), 2751–2759.
Benedicenti, S., Pepe, I.M., Angiero, F., Benedicenti, A., 2008. Intracellular ATP level increases in lymphocytes irradiated with infrared laser light of wavelength 904 nm. Photomed. Laser Surg. 26 (5), 451–453.
Bozzuto, G., Ruggieri, P., Molinari, A., 2010. Molecular aspects of tumor cell migration and invasion. Annali dell'Istituto superiore di sanita 46 (1), 66–80.
Cai, B., Ma, W., Bi, C., Yang, F., Zhang, L., Han, Z., Huang, Q., Ding, F., Li, Y., Yan, G., Pan, Z., Yang, B., Lu, Y., 2016. Long noncoding RNA H19 mediates melatonin inhibition of premature senescence of c-kit(+) cardiac progenitor cells by promoting miR-675. J. Pineal Res. 61 (1), 82–95.
Chui, C., Hiratsuka, K., Aoki, A., Takeuchi, Y., Abiko, Y., Izumi, Y., 2012. Blue LED inhibits the growth of Porphyromonas gingivalis by suppressing the expression of genes associated with DNA replication and cell division. Lasers Surg. Med. 44 (10), 856–864.
Fonseca, P.D., de Lima, F.M., Higashi, D.T., Koyama, D.F., Toginho Filho Dde, O., Dias, I.F., Ramos Sde, P., 2013. Effects of light emitting diode (LED) therapy at 940 nm on inflammatory root resorption in rats. Lasers Med. Sci. 28 (1), 49–55.
Gao, X., Xing, D., 2009. Molecular mechanisms of cell proliferation induced by low power laser irradiation. J. Biomed. Sci. 16, 4.
Giacci, M.K., Hart, N.S., Hartz, R.V., Harvey, A.R., Hodgetts, S.I., Fitzgerald, M., 2015. Method for the assessment of effects of a range of wavelengths and intensities of red/near-infrared light therapy on oxidative stress in vitro. J. Vis. Exp.(97).
Hollande, F., Pannequin, J., Joubert, D., 2010. The long road to colorectal cancer therapy: searching for the right signals. Drug Resist. Updates 13 (1-2), 44–56.
Ju, W., Wang, X., Shi, H., Chen, W., Belinsky, S.A., Lin, Y., 2007. A critical role of luteolin-induced reactive oxygen species in blockage of tumor necrosis factor-activated nuclear factor-kappaB pathway and sensitization of apoptosis in lung cancer cells. Mol. Pharmacol. 71 (5), 1381–1388.
Kalluri, R., Weinberg, R.A., 2009. The basics of epithelial-mesenchymal transition. J. Clin. Invest. 119 (6), 1420–1428.
Karu, T.I., 2008. Mitochondrial signaling in mammalian cells activated by red and near-IR radiation. Photochem. Photobiol. 84 (5), 1091–1099.
Knels, L., Valtink, M., Roehlecke, C., Lupp, A., de la Vega, J., Mehner, M., Funk, R.H., 2011. Blue light stress in retinal neuronal (R28) cells is dependent on wavelength range and irradiance. Eur. J. Neurosci. 34 (4), 548–558.
Li, X., Hou, W., Wu, X., Jiang, W., Chen, H., Xiao, N., Zhou, P., 2014. 660 nm red light-enhanced bone marrow mesenchymal stem cell transplantation for hypoxic-ischemic brain damage treatment. Neural Regen. Res. 9 (3), 236–242.
Ma, W., Ding, F., Wang, X., Huang, Q., Zhang, L., Bi, C., Hua, B., Yuan, Y., Han, Z., Jin, M., Liu, T., Yu, Y., Cai, B., Du, Z., 2018. By targeting Atg7 MicroRNA-143 mediates oxidative stress-induced autophagy of c-Kit(+) mouse cardiac progenitor cells. EBioMedicine 32, 182–191.
Mah, L.J., El-Osta, A., Karagiannis, T.C., 2010. gammaH2AX: a sensitive molecular marker of DNA damage and repair. Leukemia 24 (4), 679–686.
Mamalis, A., Garcha, M., Jagdeo, J., 2015. Light emitting diode-generated blue light modulates fibrosis characteristics: fibroblast proliferation, migration speed, and reactive oxygen species generation. Lasers Surg. Med. 47 (2), 210–215.
Markowitz, S.D., Bertagnolli, M.M., 2009. Molecular origins of cancer: molecular basis of colorectal cancer. N. Engl. J. Med. 361 (25), 2449–2460.
Neupane, J., Ghimire, S., Shakya, S., Chaudhary, L., Shrivastava, V.P., 2010. Effect of light emitting diodes in the photodynamic therapy of rheumatoid arthritis. Photodiagn. Photodyn. Ther. 7 (1), 44–49.
Niu, T., Tian, Y., Cai, Q., Ren, Q., Wei, L., 2015. Red light combined with blue light irradiation regulates proliferation and apoptosis in skin keratinocytes in combination with low concentrations of curcumin. PLoS One 10 (9), e0138754.
Oh, P.S., Na, K.S., Hwang, H., Jeong, H.S., Lim, S., Sohn, M.H., Jeong, H.J., 2015. Effect of blue light emitting diodes on melanoma cells: involvement of apoptotic signaling. J. Photochem. Photobiol. B Biol. 142, 197–203.
Oh, P.S., Hwang, H., Jeong, H.S., Kwon, J., Kim, H.S., Kim, M., Lim, S., Sohn, M.H., Jeong, H.J., 2016. Blue light emitting diode induces apoptosis in lymphoid cells by stimulating autophagy. Int. J. Biochem. Cell Biol. 70, 13–22.
Ohara, M., Kawashima, Y., Kitajima, S., Mitsuoka, C., Watanabe, H., 2003. Blue light inhibits the growth of skin tumors in the v-Ha-ras transgenic mouse. Cancer Sci. 94 (2), 205–209.
Oldenhof, H., Bisova, K., van den Ende, H., Zachleder, V., 2004. Effect of red and blue light on the timing of cyclin-dependent kinase activity and the timing of cell division in Chlamydomonas reinhardtii. Plant Physiol. Biochem. 42 (4), 341–348.
Oshima, Y., Coutts, R.D., Badlani, N.M., Healey, R.M., Kubo, T., Amiel, D., 2011. Effect of light-emitting diode (LED) therapy on the development of osteoarthritis (OA) in a rabbit model. Biomed. Pharmacother. = Biomedecine & pharmacotherapie 65 (3), 224–229.
Papageorgis, P., Cheng, K., Ozturk, S., Gong, Y., Lambert, A.W., Abdolmaleky, H.M., Zhou, J.R., Thiagalingam, S., 2011. Smad4 inactivation promotes malignancy and drug resistance of colon cancer. Cancer Res. 71 (3), 998–1008.
Rabeneck, Linda, Ann, S.H., Zauber, G., Earle, Craig, 2015. Disease control priorities, third edition. Cancer, vol. 3.
Roduit, R., Schorderet, D.F., 2008. MAP kinase pathways in UV-induced apoptosis of retinal pigment epithelium ARPE19 cells. Apoptosis 13 (3), 343–353.
Roy, N., Bommi, P.V., Bhat, U.G., Bhattacharjee, S., Elangovan, I., Li, J., Patra, K.C., Kopanja, D., Blunier, A., Benya, R., Bagchi, S., Raychaudhuri, P., 2013. DDB2 suppresses epithelial-to-mesenchymal transition in colon cancer. Cancer Res. 73 (12), 3771–3782.
Stelian, J., Gil, I., Habot, B., Rosenthal, M., Abramovici, I., Kutok, N., Khahil, A., 1992. Improvement of pain and disability in elderly patients with degenerative osteoarthritis of the knee treated with narrow-band light therapy. J. Am. Geriatr. Soc. 40 (1), 23–26.

Takhtfooladi, M.A., Shahzamani, M., Takhtfooladi, H.A., Moayer, F., Allahverdi, A., 2015. Effects of light-emitting diode (LED) therapy on skeletal muscle ischemia reperfusion in rats. Lasers Med. Sci. 30 (1), 311–316.

Teuschl, A., Balmayor, E.R., Redl, H., van Griensven, M., Dungel, P., 2015. Phototherapy with LED light modulates healing processes in an in vitro scratch-wound model using 3 different cell types. Dermatologic surgery : official publication for American Society for Dermatologic Surgery [et al.] 41(2), 261-268.

Wang, L., Hu, L., Grygorczyk, R., Shen, X., Schwarz, W., 2015. Modulation of extracellular ATP content of mast cells and DRG neurons by irradiation: studies on underlying mechanism of low-level-laser therapy. Mediators Inflamm. 2015, 630361.

Waris, G., Ahsan, H., 2006. Reactive oxygen species: role in the development of cancer and various chronic conditions. J. Carcinog. 5, 14.

Wei, E.K., Giovannucci, E., Wu, K., Rosner, B., Fuchs, C.S., Willett, W.C., Colditz, G.A., 2004. Comparison of risk factors for colon and rectal cancer. Int. J. Cancer 108 (3), 433–442.

Xu, J., Zhang, R., Zhao, J., 2017. The novel long noncoding RNA TUSC7 inhibits proliferation by sponging MiR-211 in colorectal Cancer. Cell. Physiol. Biochem. 41 (2), 635–644.

Yang, Y., Zhang, Y., Wang, L., Lee, S., 2017. Levistolide a induces apoptosis via ROS-Mediated ER stress pathway in Colon cancer cells. Cell. Physiol. Biochem. 42 (3), 929–938.

Yuan, Y., Yan, G., Gong, R., Zhang, L., Liu, T., Feng, C., Du, W., Wang, Y., Yang, F., Li, Y., Guo, S., Ding, F., Ma, W., Idiiatullina, E., Pavlov, V., Han, Z., Cai, B., Yang, L., 2017. Effects of blue light emitting diode irradiation on the proliferation, apoptosis and differentiation of bone marrow-derived mesenchymal stem cells. Cell. Physiol. Biochem. 43 (1), 237–246.